

data rates are compatible with the Multimission Spacecraft (MMS) specifications.

The changes and improvements which were incorporated into HXRBS over previous solar x-ray experiments are listed in Table 1. Another new approach taken during development

Table 1 HXRBS improvements

- 1) An increased count rate range (up to 5×10^5 counts/s).
- 2) A decrease in the effect of pulse pileup.
- 3) An increased sensitivity.
- 4) Four multiplexer tubes are summed together.
- 5) The ability to set a threshold level and require two of the four detectors to exceed it for a valid event (eliminates noise at low-activity levels).
- 6) The use of memory to accumulate time profiles of count rate activity during a solar flare.
- 7) It is operationally controlled by a spacecraft computer with occasional updates from ground control.
- 8) The use of a SIS between the instrument and the GSE permitted parallel development and utilization of both systems.

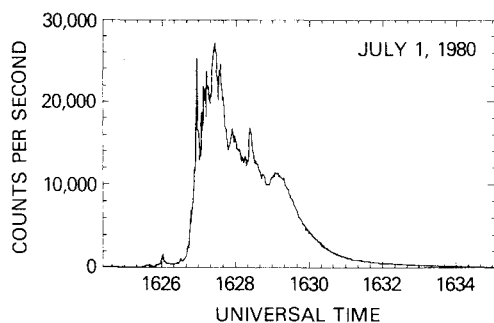


Fig. 2 Events vs time.

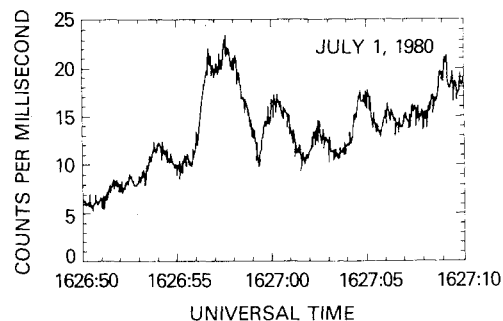


Fig. 3 Events vs time (memory).

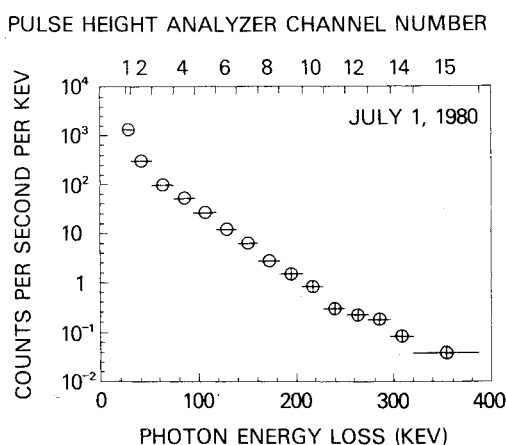


Fig. 4 Energy spectrum.

was the use of the spacecraft interface simulator (SIS). The SIS simulated the electronic signals that would be passed to the instrument by the spacecraft during flight. It also arranged the data from the instrument into a data stream identical to the data stream that was presented to the experimenter's ground support equipment (GSE) during flight. By simulating the data stream during the early stages of instrument integration, programmers were able to develop and test the GSE software using real data. Also, the integration team was able to utilize the GSE system hardware and software early in the program. Compatibility problems were thus detected and corrected very early.

Performance

At the time of this writing the HXRBS has performed flawlessly for approximately nine months. It has observed, archived, and analyzed over 1500 flares of varying magnitude and duration. Figures 2-4 illustrate typical data plots generated for each flare. This particular flare occurred July 1, 1980, and was one of the more active flares. Figure 2 is a plot of the number of valid events detected vs time. The general pattern of fast rise, followed by a second peak, and then followed by a slow decay in the count rate is typically but not exclusively the pattern of the flares seen. Figure 3 is a plot of the readout of the memory data expanded around a small section of the first peak in Fig. 2. A typical spectrum summed over an 8.192 s interval of this event is shown in Fig. 4. It indicates that most of the energy is in the lower energy channels. These spectra may be accumulated over varying periods of time as desired by the investigators.

HXRBS has not seen any evidence of count rates that exceed the maximum rate of the accumulators. It has seen very little evidence of spectral distortion or pulse pileup and has not had any hardware failures. There has been some evidence of gain changes in detector outputs, but not enough to require a change in the amplifier gains. These changes, which had been anticipated during the design of the instrument, have been due to a slight degradation of the photomultiplier tubes. This is a normal occurrence.

Reference

- ¹Frost, K., Dennis, B., and Lencho, R., "New Techniques in Astronomy," *IAU Symposium*, Vol. 41, 1971, p. 185.

AIAA 82-4177

Thermodynamics of Similar Particle-Laden Gas Flows in Convergent-Divergent Nozzles

Tarit K. Bose*

Indian Institute of Technology, Madras, India

Nomenclature

- A = cross-sectional area
 C_1-C_3 = constants
 c'' = specific heat of solid particles
 c^* = specific heat ratio = c''/c_p

Received Oct. 23, 1981; revision received Jan. 13, 1982. Copyright © American Institute of Aeronautics and Astronautics, Inc., 1981. All rights reserved.

*Professor of Aeronautical Engineering. Associate Fellow AIAA.

c_n	= polytropic specific heat of gas
c_p	= isobaric specific heat of gas
d_p	= average particle diameter
K	= u''/u'
L	= $(T_c^0 - T'')/(T_c^0 - T')$
M	= Mach number
\dot{m}	= mass flow rate
m^*	= loading ratio = $\dot{m}''/\dot{m}' = \rho'' u''/(\rho' u')$
n	= polytropic exponent for gas
Pr	= Prandtl number of gas
p	= pressure
T	= temperature
T^0	= stagnation temperature
u	= velocity
x	= axial coordinate
γ	= isentropic exponent of gas
μ	= viscosity coefficient of gas
ρ	= density
$\bar{\rho}$	= density of material of solid particles
τ	= collisional relaxation time

Subscripts and Superscripts

c	= settling chamber
t	= throat
$()'$	= gas
$()''$	= solid particles
x	= derivatives with respect to x

Introduction

RECENT interest in the development of integral solid-propellant rocket ramjets, in which a highly fuel-rich solid-propellant rocket is imbedded or attached to a supersonic combustion ramjet (scramjet) system to act as a fuel-rich hot-gas generator, has led to a renewed interest in gas-particle flows with high loading ratios.^{1,2} Analysis of such flows becomes particularly simple if we consider a steady, one-dimensional, similar flow with some other assumptions, such as, 1) there is no phase change or combustion of solid particles during the expansion process; 2) the gas is treated as ideal, $c_p = \text{const}$, $Pr = \text{const}$; and 3) the interaction between gas and particles can be described by the Stokes relation for momentum transfer and by the Nusselt relation for heat transfer for low-speed flows with the collisional relaxation time $\tau = \bar{\rho} d_p^2 / (18\mu)$ being constant along the flow. A flow is called similar if the ratio of the particle velocity to gas velocity, $K = u''/u'$, remains constant^{3,4} and smaller than one. Even in nozzles where a similarity solution is not applicable, a similar solution may precede the numerical solution to obtain required initial values.⁴ In the present Note, assumption of constant τ , in addition to the earlier assumption of similarity of flow,^{3,4} allows us to demonstrate that the gas and particle velocities increase proportional to x , the temperatures decrease proportional to x^2 , and the gas state changes with a polytropic exponent n which is constant along the flow and can be calculated. It is further shown that, depending on the loading ratio m^* the ratio of particle to gas specific heat c^* , gas acceleration, and particle size, the value of n can range between $-\infty$ to $+\infty$, except between $n=1$ and $n=\gamma$, corresponding to isobar, isochore, isotherm,⁵ and isentropic change of state.^{6,7} It is possible to show that for n between γ and 1, the polytropic specific heat of the gas c_n becomes negative, which means that there will be heat transfer during the expansion process from the gas to the particles, which is impossible. The advantage of obtaining a solution with constant n is that it is now possible to obtain closed-form solution of all flow properties and the shape of a convergent-divergent nozzle.⁶

Analysis

For steady, one-dimensional particle-laden gas flows, equations of continuity, momentum, and energy are available

for each of the particle and gas components and, globally, are about 20 in number.⁴ For the present purpose, the following equations are adequate:

Continuity:

$$\dot{m} = \dot{m}' + \dot{m}'' = (I + m^*) \rho' u' A \quad (1a)$$

Momentum:

$$\rho'' u'' u_x'' = -\rho'' (u'' - u') / \tau \quad (1b)$$

Energy:

$$\rho'' u'' (c'' T'' + u''^2/2)_x + \rho' u' (c_p T' + u'^2/2)_x = 0 \quad (1c)$$

$$\rho'' u'' (c'' T'' + u''^2/2)_x = -2\rho'' c_p (T'' - T) / (3Pr\tau) \quad (1d)$$

$$\rho'' u'' c'' T_x'' + \rho' u' c_p T_x' = u' p_x + (u'' - u')^2 \rho'' / \tau \quad (1e)$$

From definitions of K, L, m^* , and c^* as given in the Nomenclature and from Eqs. (1b) and (1c), it can easily be shown that

$$u' = C_1 x; \quad T^0 - T' = C_2 x^2$$

where

$$C_1 = (I - K) / (\tau K^2)$$

$$C_2 = [C_1^2 / (2c_p)] (I + m^* K^2) / (I + m^* c^* L)$$

Although henceforth K is taken as an independent variable and C_1 as a dependent variable, in practice C_1 , which depends on the shape of the nozzle, should be an independent variable. For a given gas exhaust velocity a larger C_1 means a shorter nozzle, and a larger τ means larger particles. From C_1 and τ one can, of course, get K as a dependent variable by solving the quadratic equation $K^2 \tau C_1 + K - 1 = 0$. It can be shown that for τC_1 small (smaller particles and small gas acceleration, large nozzle length) $K \rightarrow 1$, and for τC_1 large, $K \sim 1/\sqrt{\tau C_1}$.

Having taken K as an independent variable, L and other subsequent variables are dependent on K . Substituting above results into Eq. (1d), we get

$$L = [3Pr(I - K)K^2 + (m^* K^2 + I)] / [3Pr(I - K)c^* + (m^* K^2 + I)K] \quad (2)$$

It can now be shown that for $K=0$, $L=0$ and for $K=1$, $L=1$. For all other intermediate values of K , L also depends on m^* , c^* , and Pr .

Now formally introducing a relation for the polytropic specific heat of the gas,

$$c_n T_x' = c_p T_x' - (I/\rho') p_x$$

one can rewrite Eq. (1e) to get

$$c_n T_x' = m^* \{ [(u'' - u')^2 / (u'' \tau)] - c'' T_x'' \}$$

which further leads to the relation

$$c_n / c_p = m^* [K(I - K)(I + m^* c^* L) / (I + m^* K^2) + c^* L] \quad (3)$$

Now (c_n / c_p) is related to n as follows^{6,7}

$$n = \gamma [(c_n / c_p) - I] / [(c_n / c_p) \gamma - I] \quad (4)$$

Depending on the values of (c_n / c_p) , n can have the following values: $c_n / c_p = I$, $n=0$; $c_n / c_p = 1/\gamma$, $n \rightarrow \pm \infty$; $c_n / c_p = 0$, $n=\gamma$; and $c_n / c_p \rightarrow \infty$, $n=1$, which correspond to isobar,

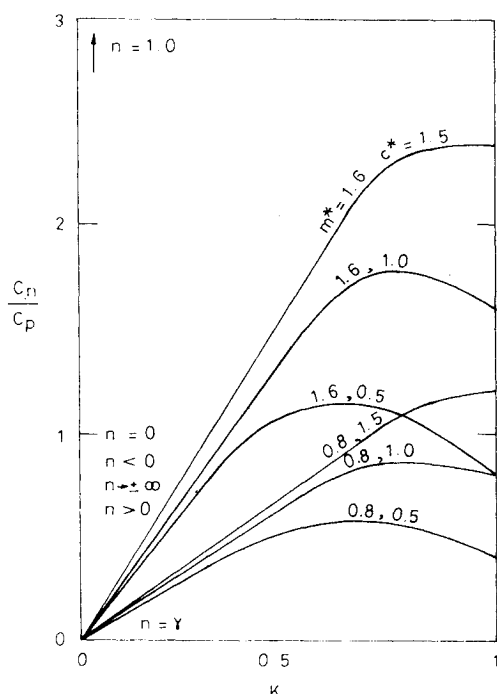


Fig. 1 Gas polytropic specific heat ratio vs similarity parameter K for different values of m^* and c^* at $Pr=0.71$, $\gamma=1.4$.

isochore, isentropic, and isotherm changes of state, respectively. The value of (c_n/c_p) , and hence n , is a function of m^* , c^* , K , γ , and Pr . Taking $\gamma=1.4$ and $Pr=0.71$, (c_n/c_p) is plotted in Fig. 1 as a function of K . It is shown that depending on m^* , c^* , and K , (c_n/c_p) can have all of the values corresponding to the above four changes of state or any intermediate values.

Now defining a gas stagnation temperature $T^0' = T' + u'^2/(2c_p)$, it is possible to show from Eqs. (1a-c) that $T^0' = T_c^0 + C_3 x^2$, where

$$C_3 = m^* C_1^2 (Lc^* - K^2) / [c_p (m^* c^* L + 1)] \quad (5)$$

It is, therefore, shown that stagnation temperature in the flow direction increases with x^2 . Finally, because of constant n during expansion, one can calculate various flow properties in the nozzle from closed-form solutions, which at the throat become⁶

$$T_c^0/T_t' = 2/(n+1); p_c^0/p_t' = (T_c^0/T_t')^{n/(n-1)}; M_t = \sqrt{n/\gamma} \quad (6)$$

References

- Thomas, A.N., "New Generation Ramjets—A Promising Future," *Astronautics & Aeronautics*, Vol. 18, June 1980, pp. 36-41, 71.
- Billig, F.S., Waltrap, P.J., and Stockbridge, R.D., "Integral-Rocket Dual-Combustion Ramjets: A New Propulsion Concept," *Journal of Spacecraft and Rockets*, Vol. 17, Sept.-Oct. 1980, pp. 416-424.
- Hassan, H.A., "Exact Solutions of Gas-Particle Nozzle Flows," *AIAA Journal*, Vol. 2, Feb. 1964, pp. 395-396.
- Soo, S.L., *Fluid Dynamics of Multiphase Systems*, Blaisdell Publishing Co., Waltham, Mass, 1967.
- Rudinger, G., "Gas-Particle Flow in Convergent Nozzles at High Loading Ratio," *AIAA Journal*, Vol. 8, July 1970, pp. 1288-1294.
- Bose, T.K., "Effect of Heat Transfer in a Converging-Diverging Nozzle," *Journal of Spacecraft and Rockets*, Vol. 4, March 1967, pp. 401-402.
- Bose, T.K., "Thermodynamic Expansion Processes for Argon Plasma in a Convergent-Divergent Nozzle," *Journal of Spacecraft and Rockets*, Vol. 10, Sept. 1973, pp. 613-615.

AIAA 82-4178

Geodetic Latitude of a Point in Space

Terrence W. Barbee*

Space Applications Corporation, Irvine, Calif.

Introduction

THE problem of computing the geodetic latitude of an arbitrary point above a reference ellipsoid has been examined by many people.¹ However, these papers were primarily concerned with obtaining approximations to geodetic latitude rather than with the exact solution. This paper presents the exact closed form solution to the problem. It is possible, however, that the ponderous form of the exact solution may not prove to be of practical use in situations where rough approximation may suffice. This Note represents the first known attempt at the exact algebraic solution.

Analytical Development

Consider the problem of finding the geodetic latitude of an arbitrary point P lying above the reference ellipsoid

$$\frac{x^2 + y^2}{a_e^2} + \frac{z^2}{b_e^2} = 1$$

where $a_e = 6378.145$ km and $b_e = 6356.759$ km. Owing to polar symmetry it suffices to restrict analysis to a meridian plane containing the point P . Let (r, z) denote the abscissa and ordinate respectively in the meridian plane so that x , y , and r are related by

$$r = \sqrt{x^2 + y^2}$$

and the ellipse under consideration is given in parametric form by

$$\begin{aligned} r &= a_e \cos t \\ z &= b_e \sin t \end{aligned} \quad -\pi/2 \leq t \leq \pi/2 \quad (1)$$

If P has Cartesian coordinates, $P = (x_0, y_0, z_0)$, then the meridian coordinates of P will be (r_0, z_0) , where $r_0 = (x_0^2 + y_0^2)^{1/2}$. Let θ denote the geodetic latitude of P . The geodetic normal through P intersects the ellipse [Eq. (1)] at some point $Q = (a_e \cos t, b_e \sin t)$, as shown in Fig. 1. The fundamental equality

$$\tan \theta = (a_e/b_e) \tan t \quad (2)$$

relates θ to t in a one-to-one manner for $t \in [-\pi/2, \pi/2]$, so that in order to determine θ it will suffice to find the value of t which defines the point Q . The two quantities, $\tan \theta$ and $(z_0 - b_e \sin t)/(r_0 - a_e \cos t)$, each represent the slope of the geodetic normal through P so that by Eq. (2),

$$z_0 - b_e \sin t = (a_e/b_e) (\tan t) (r_0 - a_e \cos t)$$

which can be written as

$$\sin t \cos t + A \cos t = B \sin t \quad (3)$$

where A and B are given by

$$A = \frac{b_e z_0}{a_e^2 - b_e^2} \quad B = \frac{a_e r_0}{a_e^2 - b_e^2} \quad (4)$$

Received July 31, 1981; revision received Dec. 1, 1981. Copyright © American Institute of Aeronautics and Astronautics, Inc., 1981. All rights reserved.

*Member of Technical Staff.